Korean J. Chem. Eng., **25**(4), 623-630 (2008)

Silicon ingot diameter modeling in Czochralski process and its dynamic simulation

Jin Soo Park*, Minkyo Seo*, Hyun Jung Oh, and Jae Hak Jung*,†**

*School of Display and Chemical Engineering, Yeungnam University,
214-1, Dae-dong Gyeongsan, Gyeongbuk 712-749, Korea
**Crystal Growth Technology, Siltron, 283, Imsoo-dong Gumi, Gyeongbuk 730-350, Korea
(*Received 30 July 2007 • accepted 1 November 2007*)

Abstract−Silicon wafers are manufactured by cutting an ingot into the same thickness. The Czochralski process is a representative method for making an ingot. During manufacture, the ingot diameter is affected by the pull speed and heat transfer amount. Therefore, controlling the ingot manufacturing process involves controlling the ingot diameter related to pull speed and controlling the heater power supply to maintain the pull speed within the allowable range. The modeling of ingot diameter can be established by the ingot pull speed change based on an understanding of the mechanism of heat transfer, and the calculation of the heat transfer amount between all the parties of the crystal growth furnace according to the energy balance equations. Comparing the simulation results with real process results, the step change of the heater showed 1st or 2nd process dynamics at all points with a time delay of 18 minutes, which was similar to that of the real process. Furthermore, the pull speed step change exhibited a 5 min time delay from the test spot, which confirmed the relation between the integral and process properties. This result is similar to the real process, too. With a specific ingot length, the temperature in each point of the furnace in the real process was similar to these simulation results.

Key words: Czochralski Process (CZ Process), Modeling, Ingot Diameter

INTRODUCTION

Over several decades, many techniques of control algorithms have been developed to control ingot diameter and pull speed of a crystal growth furnace. Advanced technologies have been applied to gain more stable work operation. Above all, fully understanding the process properties and identifying the process are required to establish these control algorithms. Generally, all control algorithms verify the process and identify it by defining the process parameters.

Due to the economic and technological limits, process tests are very limited, so a minimum number of simple tests are used to determine all process properties. These situations reduce the reliability of process identification and cause financial damage by experiments to determine process identification.

In the Czochralski process, the dynamic trace of ingot diameter depends on the pull speed and the heat transfer.

The aim of this study was to establish the exact modeling of ingot diameter by ingot pull speed change and to understand the heat transfer mechanism. To calculate the heat transfer amount effectively, we focused on radiation and conduction that happen mostly in the Czochralski process. Thus, the zone method was used to calculate radiation [1-3]. This method divides a curved surface into many small surfaces to calculate easily the radiation. Radiation between small flat surfaces is calculated by the zone method and radiation is summed up between small flat surfaces to get the total radiation. In case of conduction, an energy balance is used to calculate the heat transfer between the graphite crucible and quartz crucible, quartz crucible and melt, melt and ingot.

If precise modeling which considers the variables affecting the Czochralski process is developed by computer simulation, then process identification experiments could be run irrespective of the number of times. Though we tested the modeling instead of a real process, we can know how well the control algorithm can be applied, and how well control parameters were optimized according to the simulation results of the modeling. In addition, we can reduce economic damage and minimize the number of actual test.

INGOT DIAMETER MODELING AND SIMULATION OF CRYSTAL GROWTH FURNACE

In the control process of the crystal growth furnace, pull speed and ingot diameter are control variables, while the tuning variables which have to be tuned to manage control variables are the electric energy in the heater and the pull speed. Therefore, the dynamic trace of ingot diameter depends on the pull speed and heat transfer.

The necessary constants to perform modeling on the crystal growth furnace are the weight and size of the device itself, the materials and property. The pull speed and relations between the crystallization interface temperatures of the melt are also essential factors. The variation of cooling water temperature is fixed to the process. The crucible rotation, and the direction and intensity of induction are exceptions to the parameters. Therefore, we assumed that ingot diameter was affected by the heat transfer and pull speed [4]. The graphite shield effect is also very important. In this paper we newly suggest the model of crystal growth furnace with shield element. Fig. 1 shows the crystal growth furnace model and the modeling phase.

1. Heater surface radiates heat to the surface of the graphite crucible.

2. Heat is transferred by conduction to the quartz crucible which touches the graphite crucible.

3. Quartz crucible transfers heat to poly silicon melt by conduc-

†To whom correspondence should be addressed.
E-mail: jhjung@yumail.ac.kr

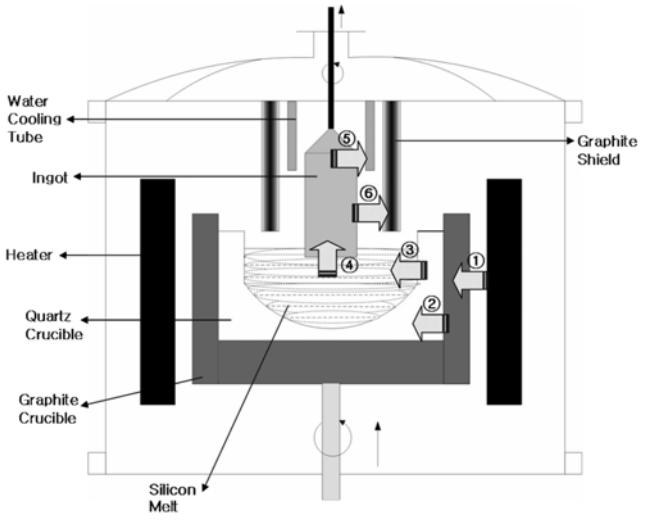

Fig. 1. Design of the crystal growth furnace and modeling phase.

tion. The average melt temperature is calculated by the melt volume and the amount of heat transferred by the quartz crucible.

4. Heat transferred to the crystallized ingot from the melt is determined by heat conduction between the ingot and melt. The radiation heat from the melt to ingot is ignored.

5. Heat transfers to the cooling water tube from surface of the crystallized ingot by radiation.

6. Heat transfers between the surface of the crystallized ingot and the graphite shield by radiation.

7. Crystal growth diameter is determined by the moment speed and temperature of the melt right after the heat transfer sequence of the first iteration.

Determining the dynamics of crystal growth according to the above modeling sequence requires effective calculation of energy transfer. The system geometry is important in the crystal growth furnace process in which radiation occurs mostly. In this modeling, Monte Carlo simulation was used to calculate the radiant energy. Eq. (1) is a radiation equation.

$$\text{View Factor: } F_{12} = \frac{1}{A_1}\int_{A_1}\int_{A_2} \frac{\cos\phi_1 \cos\phi_2}{\pi s_1^2} dA_1 dA_2$$

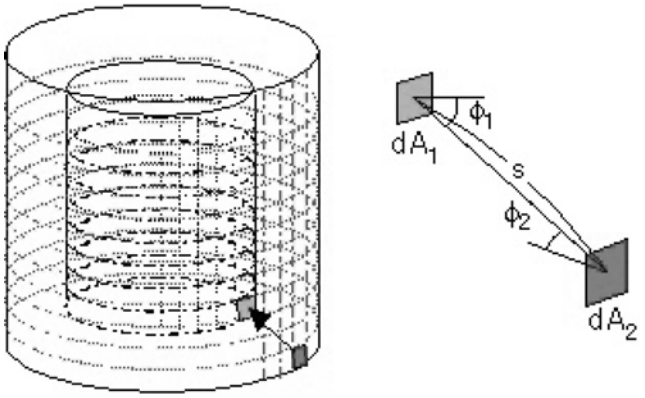

Fig. 2. Surface divided by zone method.

$$Q_{12} = \sigma A_1 F_{12}(T_1^4 - T_2^4) \quad (1)$$

As shown in Eq. (1), the zone method is used in this research to calculate the radiant energy. This method divides a curved surface into many small surfaces to calculate easily the view factor, thereby yielding the total heat transfer by uniting after the radiant energy between small surfaces is calculated. The heater, graphite crucible and cylinder shaped cooling water tube are divided into small flat surfaces attached to a cylinder vertical to the tangential line. The radiation between the small flat surfaces which do not confront each other is calculated to obtain the sum of total heat transfer. The total heat transfer by radiation is calculated with this method.

1. Calculating Radiation between Unit Flat Surfaces

In case of radiation, because the furnace pressure is maintained around 100 torr, we suppose that the furnace is nearly a vacuum. Thus, we ignore radiation damage by air density.

To calculate the radiant energy between the unit surfaces of a graphite crucible divided by zone method, we must calculate a view factor between unit surfaces. To perform the calculation, the view range of the unit surface factor of graphite (dA_1) to each unit surface (dA_2), ϕ_1 and ϕ_2 is required. These are the angles between the line extended from the two unit surfaces and each surface's normal line. Fig. 3 is the grower's plane figure. The red curve of the heater is the view angle of one unit flat surface of graphite which can absorb radiation. ϕ_1 and ϕ_2 are decided by ϕ_0. The range of ϕ_0 is $0<\phi_0<\cos^{-1}(R_1/R_2)$, when the view range of heater radiation is from a to b. The number of unit surfaces per vertical surface of the heater is decided by the number of equally divided ϕ_0 in this range. The width of the unit surface can be approximately determined by the unit angle of ϕ_0 when equally divided.

As shown in Fig. 3, when the unit angle gets narrower, each arc of the heater and graphite becomes straight line c and d; however, if we carry on the division too many times, then the number of the unit surface increases which increases the computation time.

$$\Delta h = \frac{H}{N}, \qquad \Delta g = \frac{G}{M}$$

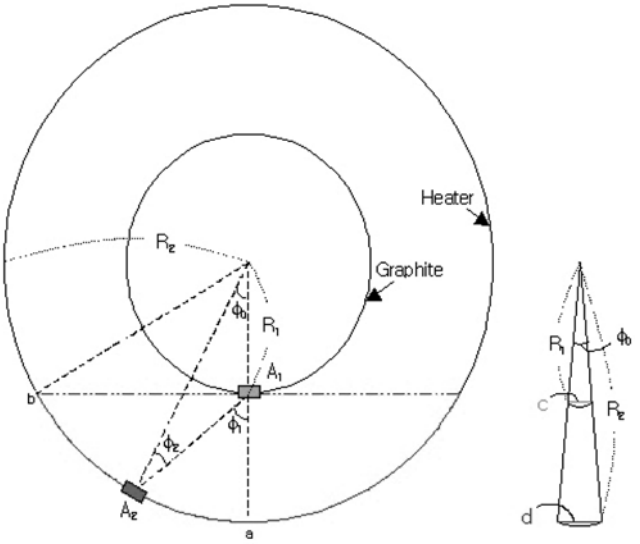

Fig. 3. ϕ_1, ϕ_2 between unit the flat surfaces.

Δh is the unit height of heater, H is heater height and Δg is the unit height of graphite, G is graphite height. Then the size of each unit surface A_1 and A_2 is:

$A_1=\Delta g\times c, \quad A_2=\Delta h\times d$

Fig. 3 is a plane figure and Fig. 4 is a 3-dimensional figure to represent the visual range of ϕ_0. The double amount of heat received from the heater surface in the range of a-b is the total heat of the graphite crucible's unit surface within the visual range of radiation.

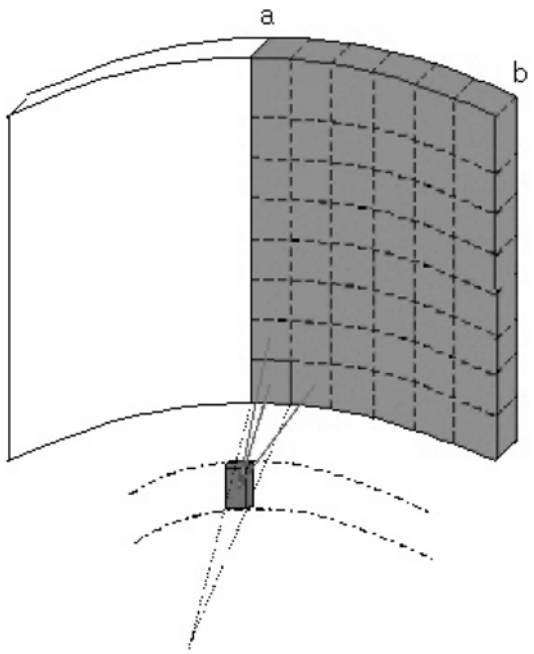

Fig. 4. 3-Dimensional drawing between unit flat surfaces.

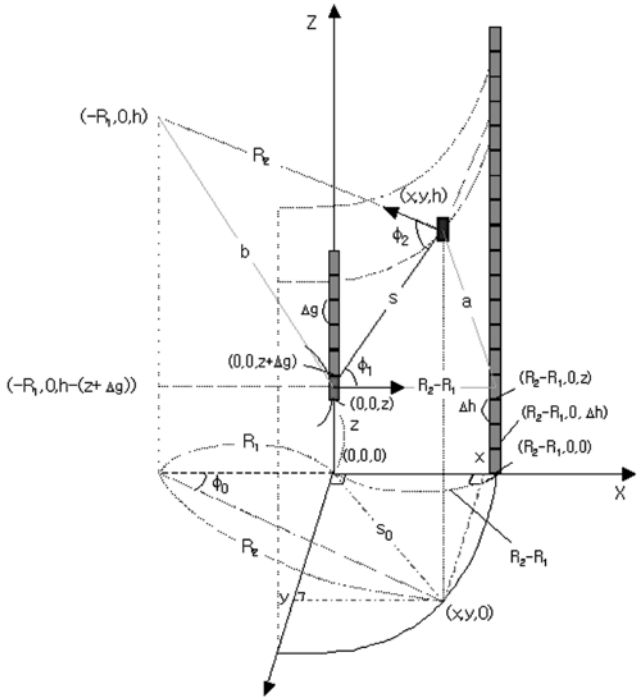

Fig. 5. Establishing coordinates per unit flat surface.

To obtain ϕ_1 and ϕ_2 for calculating the view factor and s (distance between two unit surfaces), the geometry is displayed in Fig. 5 with 3 dimensional coordinates. Each unit surface's coordinates were calculated by using the lowest unit surface of the graphite crucible as a datum point. According to the trigonometric function formula, S_0 is given by Eq. (2):

$$S_0=\sqrt{R_1^2+R_2^2-2R_1R_2\cos\phi_0} \tag{2}$$

Therefore, x and y are

$$y=R_2\sin\phi_0, \quad x=\sqrt{s_0^2-y^2}$$

According to the trigonometric function formula, if each point's coordinates are known, then the distance between two points can be calculated and thereby the angles between them can also be calculated. The formula is as follows:

$$\text{Distance between two points}=\sqrt{(x_2-x_1)^2(y_2-y_1)^2+(z_2-z_1)^2}$$

$$\text{Angle between line a and b}=\cos^{-1}\left(\frac{a^2+b^2-c^2}{2ab}\right) \tag{3}$$

Therefore, the equation that evaluates the unknown variable s (distance between two unit surfaces), a, b, ϕ_1 and ϕ_2 can be expressed according to Eq. (3), where *s* is the distance between the unit surface coordinates of the heater (x, y, h) and those of the graphite crucible (0, 0, z+Δg), a is the distance between (x, y, h) and (R_2-R_1, 0, z), and b is the distance between ($-R_1$, 0, h) and (0, 0, z+Δg).

$$s=\sqrt{x^2+y^2+(h-(z+\Delta g))^2}$$

$$a=\sqrt{(x-(R_2-R_1))^2+y^2+(h-(z+\Delta g))^2}$$

$$b=\sqrt{(-R_1)^2+(h-(z+\Delta g))^2}$$

ϕ_1 is the angle between *s* and (R_2-R_1) in triangle (s~(R_2-R_1)~a)

$$\phi_1=\cos^{-1}\left(\frac{s^2+(R_2-R_1)^2-a^2}{2s(R_2-R_1)}\right)$$

ϕ_2 is the angle between s and R_2 in (s~R_2~b),

$$\phi_2=\cos^{-1}\left(\frac{s^2+R_2^2-b^2}{2sR_2}\right)$$

The radiation heat and view factor between each unit surface can be calculated by using Eq. (1). The radiated heat quantity that is transferred to the graphite crucible from the heater follows this procedure.

(i) The unit surface of the graphite (when y=0) is the datum line of all calculations. When the unit surface coordinate is y=0 (R_2-R_1, 0, h), the radiant energy that a unit surface of the graphite receives from all the unit surface lines located in axis x is calculated.

(ii) while ϕ_0 changes to a certain unit angle in the range of $\{0<\phi_0<\cos^{-1}(R_1/R_2)\}$, double the heat that a unit surface of graphite receives from all heaters that are in range of ϕ_0.

The heat from (ii) plus the heat from (i) gives the total heat that a unit surface of graphite receives in the range of all view range.

(iii) Repeat (i) and (ii) for all other unit surfaces which have a value of 0 in axis y. The sum of the heat for each unit surface is the heat for one column in the divided graphite crucible.

(iv) The number of all graphite lines is decided when 360° is di-

vided by the unit angle. The number of all graphite lines multiplied by the heat from (iii) is the heat that the graphite crucible obtains from the heater.

2. Heat Conduction Energy Balance

The heat transfer between the graphite crucible and quartz crucible, quartz crucible and melt, and melt and ingot is carried by conduction, and can be calculated by Eq. (4):

$$Q=UA(T_1-T_2) \tag{4}$$

The total heat transfer (Q) is correlated with the heat transfer coefficient (U), contacting area (A) and temperature difference between the two contacting materials (T_1-T_2). The average temperature of the melt, which is calculated by using the total quantity of melt, is easily determined in the heat transfer by conduction [5,6].

The energy balance between the heater, graphite crucible, quartz crucible, melt, ingot and graphite shield is given by:

$$\frac{dQ}{dt}=Q_{input}-Q_{output}$$

$$\frac{m_1Cp_1dT_1}{dt}=A_0F_{01}(T_0^4-T_1^4)-U_1A_1(T_1-T_2) \quad \cdots\cdots \text{①}$$

$$\frac{m_2Cp_2dT_2}{dt}=U_1A_1(T_1-T_2)-U_2A_2(T_2-T_3) \quad \cdots\cdots \text{②}$$

$$\frac{m_3Cp_3dT_3}{dt}=U_2A_2(T_2-T_3)-U_3A_3(T_3-T_4) \quad \cdots\cdots \text{③}$$

$$\frac{m_4Cp_4dT_4}{dt}=U_3A_3(T_3-T_4)+A_4F_{46}(T_4^4-T_6^4)-A_4F_{45}(T_4^4-T_5^4) \quad \cdots \text{④}$$

The value of T in the right side is actually $T_i=f(t)$, but, for a short time T may be considered constant.

① $\int m_1Cp_1dT_1=\int\{A_0F_{01}(T_0^4-T_1^4)-U_1A_1(T_1-T_2)\}dt$

$\rightarrow m_1Cp_1(T_1^2-T_1^1)=A_0F_{01}(T_0^4-T_1^4)(t_2-t_1)-U_1A_1(T_1-T_2)(t_2-t_1)$

② $m_2Cp_2(T_2^2-T_2^1)=U_1A_1(T_1-T_2)(t_2-t_1)-U_2A_2(T_2-T_3)(t_2-t_1)$

③ $m_3Cp_3(T_3^2-T_3^1)=U_2A_2(T_2-T_3)(t_2-t_1)-U_3A_3(T_3-T_4)(t_2-t_1)$

④ $m_4Cp_4(T_4^2-T_4^1)=U_3A_3(T_3-T_4)(t_2-t_1)$

$+A_4F_{46}(T_4^4-T_6^4)(t_2-t_1)-A_4F_{45}(T_4^4-T_5^4)(t_2-t_1)$

3. Calculating the Contact Area between Si-melt and Quartz Crucible

In ② and ③ of the above energy balance equation, the heat transfer Q $\{Q=U_2A_2(T_2-T_3)\}$ between the quartz crucible and Si-melt by conduction is transferred through contact area (A_2). As the ingot grows, the volume of melt shrinks. Therefore, the variation of contact area (A_2) must be considered and the surface of the Si-melt must be in a constant position in order for the furnace to be lifted as the melt shrinks. The height of the Si-melt was impossible to obtain in the actual process so the injected weight of silicon nugget was converted into the weight of the silicon melt in order to calculate the initial mass of the melt. The contacting melt height and quartz decrease because the melt shrinks as the ingot grows.

Therefore, the remaining volume of the melt is the difference between the initial melt volume and the growing volume of the ingot, as shown in Fig. 6.

(i) In case the melt volume$\geq(2/3)\pi R_a^3$ (Volume of hemisphere)

The melt height is calculated using volume

volume of melt=volume of hemisphere$+\pi R_a^2$meltH_1

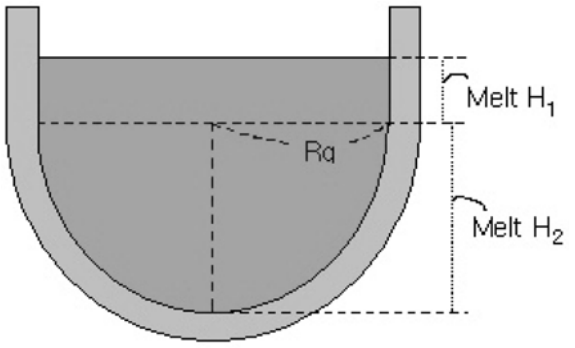

Fig. 6. Defining contacting area of melt-quartz and melt height.

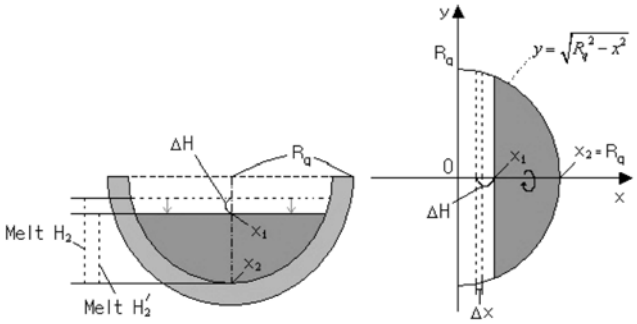

Fig. 7. Calculation of mass of melt using numerical integral.

$$\text{melt } H_1=\frac{\text{volume of melt}-\text{volume of hemisphere}}{\pi R_a^2}$$

∴ Melt height=R_a+melt H_1

∴ Contact area: $S=2\pi$ melt H_1

(ii) In case the melt volume$\leq(2/3)\pi R_a^3$ (volume of hemisphere)

When the remaining volume of melt is smaller than the volume of the hemisphere, the variation between the decreased melt and initial melt (ΔH) must be known. The furnace must be lifted as the melt shrinks because melt surface must be maintained in a constant position. To reveal this height, a numerical integral was used. To perform the numerical integral, the interval (Δx) must be fixed at a very small value. As a result of an experiment when Δx was 0.001, we obtained an approximate value within an appropriate computing time. The numerical integral is expressed below.

- Mass of used melt: $V\cong\sum_{n=1}^{\infty}\pi(\sqrt{R_a^2-(n\cdot\Delta x)^2})^2\cdot\Delta x$

The count of the number of iterations when the actual mass of the used melt becomes the value from the numerical integral. Therefore, the decreased height ΔH is:

- $\Delta H=\Delta x\times$the number of iteration

The height of the latter melt is:

- new Melt H_2'=former Melt $H_2-\Delta H$ and $x_1=R_q-$Melt H_2'

The contact area of the melt is calculated by using the surface area of a sphere formula:

$$\text{If } y=\sqrt{a^2-x^2},\ \text{then } S=2\pi\int_{-a}^{a}y\cdot\sqrt{1+y'^2}dx=2\pi a\int_{-a}^{a}dx=4\pi a^2$$

Therefore,

• The contact area of the melt is:

$$2\pi R_a \int_{x_1}^{x_2} dx = 2\pi R_a x_2 - 2\pi R_a x_1 = 2\pi R_a^2 - 2\pi R_a x_1$$

4. Heat Transfer between Melt and Ingot

To identify the process, the pull speed and variation of ingot diameter according to changes in the heater temperature were the main focus in this study, so only the main heat transfer, rather than all interactive heat transfer, was considered. The pull speed and the equation that is determined by temperature were obtained by deriving the equation that can gain the diameter by using the melt temperature and the pull speed of that time. The ingot crystallization equation suggested in this paper about average temperature and pull speed originated in the study of Kim [1], but Kim's method was targeted at the 125 mm diameter ingot. Especially, the pull speed related to the effect of ingot diameter was not an influencing feature of the operation process. Therefore, the basic pull speed, melt temperature and simplified relation equation of the ingot diameter were referred and the numerical formula was derived by considering the features of the operation process.

The term which the pull speed affects the diameter is the V-equation, while that which the temperature affects the diameter is the T-equation.

In addition, the process dynamics which show the variables of diameter while the temperature of melt changes affected by the heater's temperature do not reflect the process dynamics. However, the differential equation of multilevel heat transfer which originated from the Monte Carlo simulation developed in this study explains the result well. In the experimentally materialized integral process which has a time delay, the simulation was developed to reflect all dynamics.

The basic pull speed and effect of the ingot diameter by the melt temperature are expressed by the following Eq. (5):

$$\text{V-equation} = \left(\frac{1}{V + 0.4} - 0.888\right) \times 2 \tag{5}$$

In this Eq. (5), V is the actual operational pull speed, and the *operation* data unit is [mm/min] in 1 minute sampling time. According to the actual data, the range of V is 0.5-1.1 mm/min so the range of V-equation is −0.442-0.446 cm.

Compared to the temperature effect, the effect of pull speed does not affect the diameter greatly so we considered this point.

$$\text{T-equation} = \left(\frac{10}{\sqrt{\Delta T + 500}} - 0.39\right) \times 60 \tag{6}$$

ΔT is the difference between melting point of silicon (1,412 °C) and the average melt temperature. Computer simulation gives a range of ΔT of 5-200 °C. Therefore, the ingot diameter is scaled to have a range of fluctuating at ±3.4 cm while the temperature changes 1-400 °C.

As shown in Eq. (7), for that reason, the variation of diameter is expressed with pull speed and temperature.

$$R_2' = 7.752 + \left(\frac{1}{V + 0.4} - 0.888\right) \times 2 + \left(\frac{10}{\sqrt{\Delta T + 500}} - 0.39\right) \times 60 \tag{7}$$

When pull-speed=0.6 and ΔT=50, the theoretical diameter is almost constant so the value of 7.752 is fixed to the ingot radius of 10.16 cm.

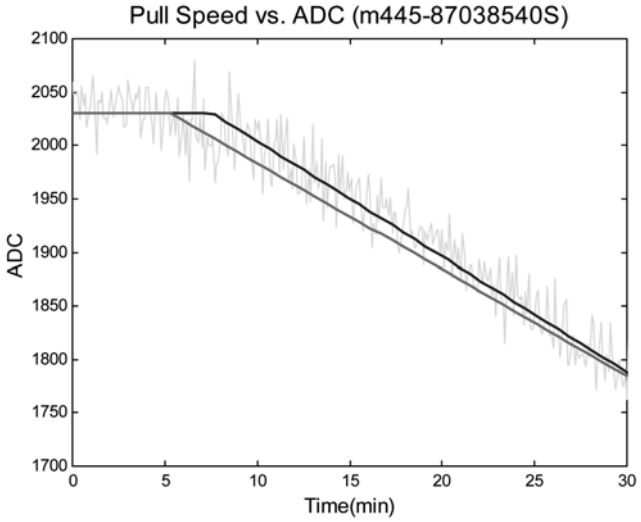

Fig. 8. Response of diameter as pull speed's step-up varies.

The above equation does not consider the dynamics of ingot diameter as the pull speed changes because it only considers the effect of the present pull speed.

We gained the dynamics as shown in the Fig. 8 from the experimental result of the ingot diameter movements for a pull speed with a step change of 0.03 mm/min up from the steady-state.

Fig. 8 shows the response of the actual diameter and that of the presumed model when pull speed was stepped up to 0.03 mm/min. The pull speed vs. dynamic characteristics of the diameter were well expressed with the integral process, which has a time delay, and the model parameter where the uncertainty is considered a test was presumed as shown below.

$$G_P = -\frac{k}{s} e^{-\theta s}$$

$$265.34 < k\left(\frac{DIA_{scaled}}{mm}\right) < 360$$

$$5.2 < \theta < 7.2$$

In this research which focused on the dynamics of pull speed, also considered was the effect of diameter which is affected by the diameter of ingot expectation and the integral calculus process. The dynamic equation is shown below.

$$G_P = -\frac{265.34}{s} e^{-5.2s}$$

It considers the integral process which has a 5.2 min time delay and −265.34(DIA_{scaled}/mm) gains. Eq. (8) is the final ingot diameter formula, which reflects the integral process that regards the pull speed trajectory as the pull speed of steady-state to ingot diameter.

$$R_s = 7.752 + \left(\frac{1}{V_{st} + 0.4} - 0.888\right) \times 2 + \left(\frac{10}{\sqrt{\Delta T + 500}} - 0.39\right) \times 60 + \Delta R_s \tag{8}$$

V_{st} means the value of the exemplary pull speed within a given time, and ΔR_s the error of R_s which is the actual pull speed acting

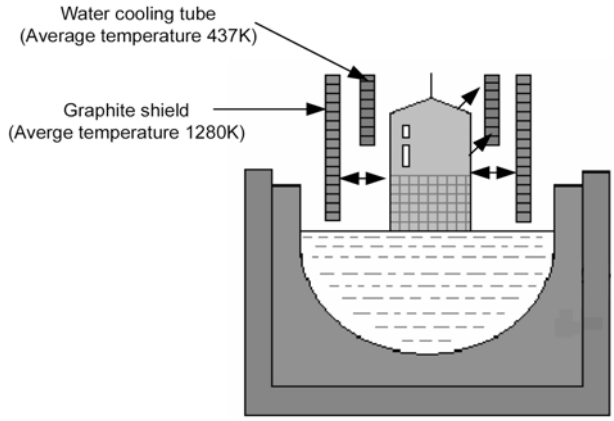

Fig. 9. Growth of ingot, cooling water tube and radiation between the ingot and graphite shield.

as the input in the integral calculus process.

The R_s shows the radius of the ingot diameter in cm units. This equation is combined with the energy simulation model ①-⑤ to give an equation that reveals the dynamics in diameter according to changes in the pull-speed trajectory, and temperature trajectory of the heater in real-time process.

5. Radiation between Ingot and Water Cooling Tube, Ingot and Graphite Shield

If the pull speed data is 0.5 mm/min at one point of the sampling time process data, 1 iteration is assumed for 1 minute. The minimum ingot growth is set to 0.1 mm for the computer simulation because the radiation is calculated by the zone method. If the ingot grows by 0.5 mm per minute, then the cell grows by 5 after each iteration. Each section of the ingot temperature has a different value, because as the ingot grows the ingot temperature is cooled by cooling water. However, the required computational capacity to calculate that is impossible. Therefore, in this study we assigned the ingot temperature calculated by heat transfer calculation as the average temperature.

According to company A lab's temperature table, the average temperature of the cooling water tube and graphite shield was 437 K and 1,280 K, respectively. In this study, we fixed the temperature of the cooling water tube at 437 K and the graphite shield at this value.

The cooling water tube cools the ingot while the graphite shield warms the ingot, when it is cooler than the graphite shield but cools the ingot when the graphite shield is cooler. The graphite shield plays an important role because the graphite temperature difference between the ingot and cooling water will be huge. Theoretically, the heat capacity transferred to the cooling water tube becomes huge too, so that the ingot temperature approaches that of the cooling water tube. This phenomenon has a gap with the actual process; thinking of the graphite shield as the grower's thermostat and the heat transfer between ingot and cooling water tube makes modeling more actual.

DYNAMIC SIMULATION RESULTS

Fig. 10 shows the heat balance from the heater to cooling water tube and the result of the dynamics simulation test. Fig. 10 shows the power supply line in an ideal process situation and the variation of diameter as the ingot grows while maintaining a constant growth at 10 cm. With this modeling simulation, we tested the variation of ingot diameter of two types of step change. Fig. 11 shows the effects of step change (+50 K) after 200 iterations (ingot body growth 172.4 mm) and Fig. 12 shows the power step change of the real process.

These two results show the typical form of low iteration which approaches the next steady state after a certain time. Moreover, their time delay is 15minutes.

Fig. 13 shows the results of the power step change down (–50 K) at 300 iterations and step change up (+50 K) at 800 iterations.

Fig. 14 shows the pull speed step change up (+0.3 mm/min) at 300 iterations.

As shown in these results, this simulation shows the dynamic ingot diameter which is affected by the pull speed and the heat ac-

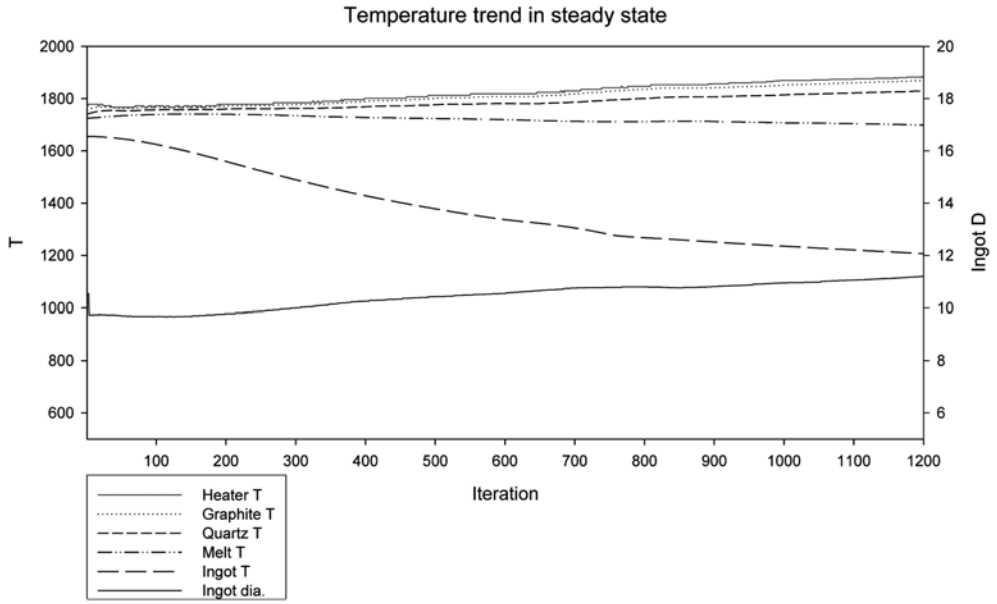

Fig. 10. Ingot diameter trend in steady state.

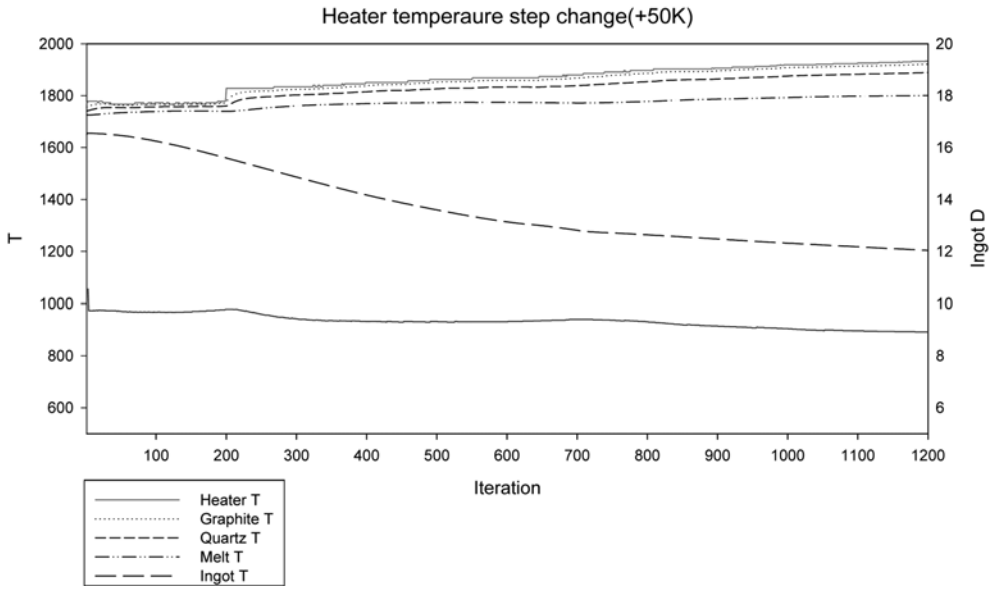

Fig. 11. Ingot diameter trend at temperature step change (+50 K).

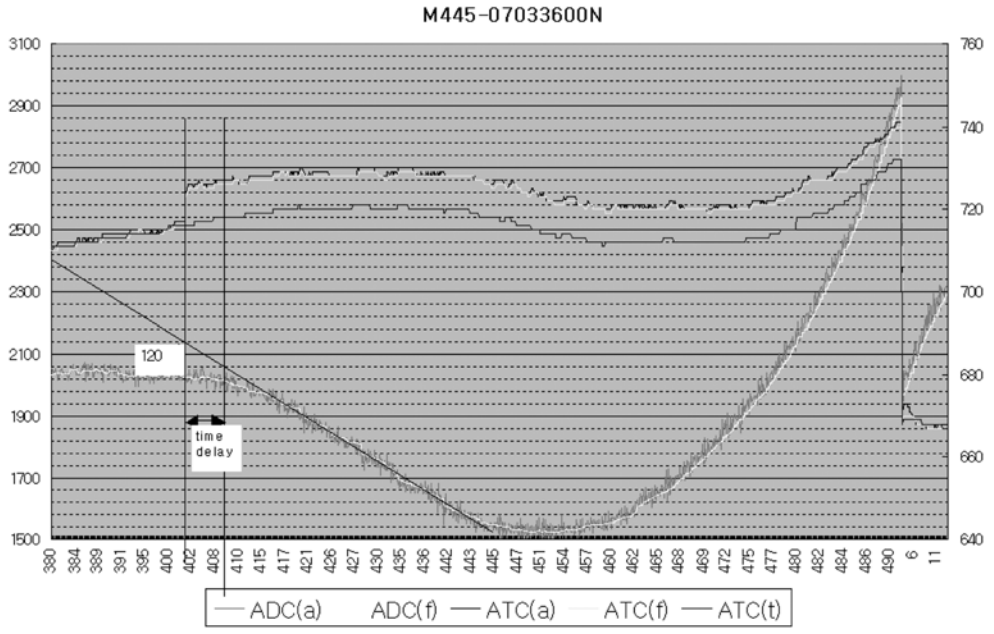

Fig. 12. Power step change at actual process.

cumulation. This modeling appears to explain the real process trend very well. So this research should be useful for operators in the real field to predict the ingot diameter dynamics with controlling heater level and pull speed change.

CONCLUSION

A step change test of heater level and pull speed was performed at various points to determine the degree of agreement between this simulation and the real system.

The test results indicated that the step change of the heater showed regular process dynamics at all points and that the time delay was 18 minutes, which is similar to that of the real process. Furthermore, the pull speed step change exhibited a 5 [min] time delay from the test spot, which confirms the relation between the integral and process properties. With a 390 mm ingot length, company A lab's simulation results for the temperature of the inner spots were similar to those of this study.

Table 1 shows the average temperature of ingot length (390 mm) for each sector according to company A lab's result. This modeling has many assumptions and errors. Nevertheless, considering all the results, the variation trend of ingot diameter (such as pull speed and temperature of heater shifts) well explains the actual process. Using this simulation promises to reduce the ingot errors and time. Finally, the identification data are attributed to the parameter tuning of the process control.

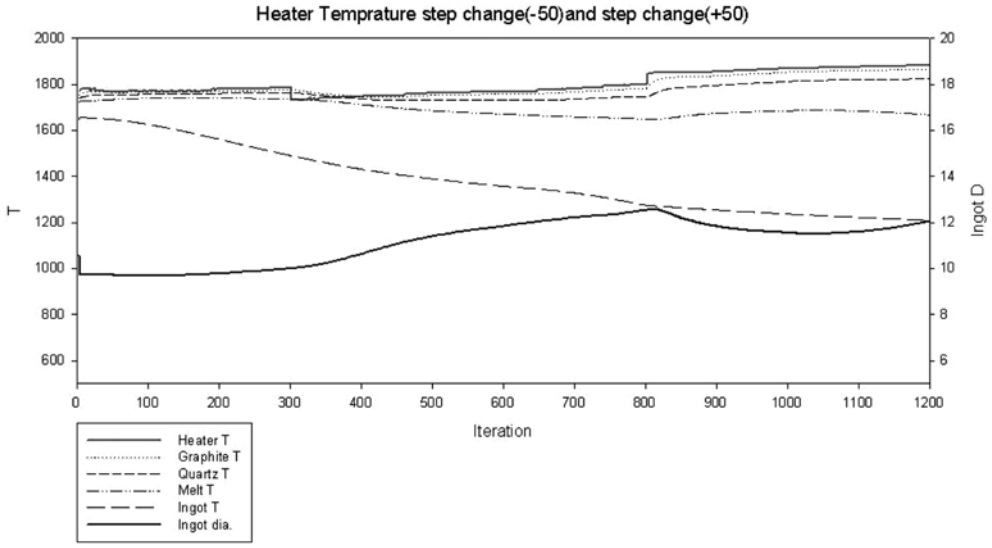

Fig. 13. Ingot diameter trend at temperature step change (−50 K after +50 K).

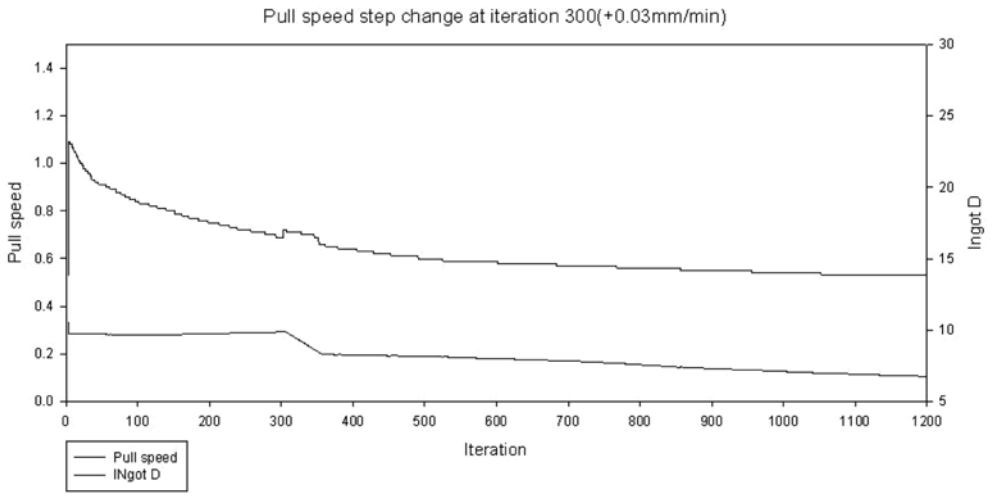

Fig. 14. Ingot diameter trend at pull speed step change (+0.03 mm/min).

Table 1. Average temperature of ingot length (390 mm) for each sector

	Lab. result	Paper result
Avg. temp. heater (K)	1836.7	1836.7
Avg. temp. graphite crucible (K)	1802.5	1812.4
Avg. temp. quartz crucible (K)	1793.9	1789.7
Avg. temp. melt (K)	1742.6	1750.3
Avg. temp. ingot (K)	1360.8	1371.1

ACKNOWLEDGMENT

This research was supported by the Yeungnam University research grants in 2007.

REFERENCES

1. J. H. Kim, D. K. Lee, Y. J. Kim, J. H. Jung, M. Y. Lee, J. G. Park and J. K. Sohn, *Theories and Applications of Chem. Eng.*, **5**(2), 2481 (1999).
2. D. K. Lee, J. H. Jung, M. Y. Lee, J. G. Park and J. K. Sohn, *Theories and Applications of Chem. Eng.*, **6**(2), 597 (2000).
3. M. K. Seo, Y. J. Kim, J. H. Jung and M. Y. Lee, *Theories and Applications of Chem. Eng.*, **7**(1), 597 (2001).
4. B. W. Bequette, *Process dynamics modeling analysis and simulation*, Prentice-Hall, Inc. New Jersey (1998).
5. J. M. Smith, H. C. Van Ness and M. M. Abbott, *Introduction to chemical engineering thermodynamics 6th edition*, McGraw-Hill Korea, Seoul (2003).
6. W. L. McCabe, J. C. Smith and P. Harriott, *Unit operation of chemical engineering 6th edition*, McGraw-Hill Korea, Seoul (2003).
7. J. H. Wang, J. I. Im and K. H. Lee, *Korean J. Chem. Eng.*, **21**, 1231 (2004).
8. H. M. Lee, K. J. Lee and S. Y. Hahn, *Korean J. Chem. Eng.*, **6**, 105 (1989).